CO_2 laser pulse shortening by laser ablation of a metal target

T. Donnelly, M. Mazoyer, A. Lynch, G. O'Sullivan, F. O'Reilly, P. Dunne, and T. Cummins

Citation: Review of Scientific Instruments **83**, 035102 (2012);
View online: https://doi.org/10.1063/1.3690066
View Table of Contents: http://aip.scitation.org/toc/rsi/83/3
Published by the American Institute of Physics

CO_2 laser pulse shortening by laser ablation of a metal target

T. Donnelly, M. Mazoyer, A. Lynch, G. O'Sullivan, F. O'Reilly, P. Dunne, and T. Cummins
School of Physics, University College Dublin, Belfield, Dublin 4, Ireland

(Received 30 November 2011; accepted 20 February 2012; published online 5 March 2012)

A repeatable and flexible technique for pulse shortening of laser pulses has been applied to transversely excited atmospheric (TEA) CO_2 laser pulses. The technique involves focusing the laser output onto a highly reflective metal target so that plasma is formed, which then operates as a shutter due to strong laser absorption and scattering. Precise control of the focused laser intensity allows for timing of the shutter so that different temporal portions of the pulse can be reflected from the target surface before plasma formation occurs. This type of shutter enables one to reduce the pulse duration down to ∼2 ns and to remove the low power, long duration tails that are present in TEA CO_2 pulses. The transmitted energy is reduced as the pulse duration is decreased but the reflected power is ∼10 MW for all pulse durations. A simple laser heating model verifies that the pulse shortening depends directly on the plasma formation time, which in turn is dependent on the applied laser intensity. It is envisaged that this plasma shutter will be used as a tool for pulse shaping in the search for laser pulse conditions to optimize conversion efficiency from laser energy to useable extreme ultraviolet (EUV) radiation for EUV source development. © *2012 American Institute of Physics*. [http://dx.doi.org/10.1063/1.3690066]

I. INTRODUCTION

High power pulsed CO_2 lasers are widely used for a host of industrial processes and research applications. Due to the available high peak power and electrical efficiency they are commonly used for laser cutting, machining, and microengineering as well as production of hot plasma for materials deposition, x-ray emission and ion sources. CO_2 lasers commonly employ the transverse electric atmospheric (TEA) configuration, which consists of a pulsed electrical discharge through a gaseous laser medium close to atmospheric pressure generating a high power laser pulse. The laser gas medium is usually a combination of CO_2, N_2, and He and their relative abundance determines the laser pulse energy and temporal profile.

CO_2 lasers are expected to play a crucial role in the realization of commercially viable extreme ultraviolet (EUV) emitting sources for semiconductor lithography.[1] This is partly due to the favorable opacity conditions that result in enhanced EUV emission when laser produced plasmas (LPPs) are formed with far infrared laser irradiation compared with those formed using optical and near infrared lasers.[2] LPP emission in a 2% band centered on 13.5 nm is the leading candidate as the source for next-generation photolithography in high-volume manufacturing of computer processors and memory components.[1] To optimize the EUV emission, the tin LPP should have an electron temperature in the region of 35 eV, where the dominant ions are Sn^{8+} to Sn^{10+}, resulting in a narrow band of bright emission at 13.5 nm. Plasma opacity reduces the brightness of this emission when the plasma electron density exceeds 10^{19} cm^{-3}. The long wavelength (10.6 μm) of CO_2 laser radiation ensures that the LPP electron density is below 10^{19} cm^{-3} and that the plasma is essentially optically thin to 13.5 nm radiation.

The high electrical efficiency of CO_2 lasers also makes them favorable for integration into semiconductor high volume manufacturing (HVM). The HVM suitable CO_2 lasers are still under development,[3] but TEA CO_2 lasers are routinely used for research studies into the EUV emission of LPPs. However, a TEA CO_2 laser temporal profile is characterized by an initial large peak of 50–100 ns pulse duration, followed by a low energy, 1–2 μs tail. The presence of a small amount (10%) of N_2 in the gas mix allows for improved excitation of the upper level of the CO_2 molecule thus increasing the energy yield from the lasing process, but N_2 also has a longer de-excitation time, resulting in the low energy tail that follows the initial laser pulse peak. A large portion (30%–50%) of the energy contained in the laser pulse is in this tail. An example of a TEA CO_2 laser pulse profile is shown in Fig. 1 where the initial peak (1) and the long tail (2) are marked. The laser pulse temporal profile is problematic for two reasons. First, it is difficult to assign a meaningful power density value to the overall pulse. This issue is further compounded by the oscillatory nature of the pulse power during the laser pulse. Second, the low energy tail is of insufficient power to sustain the high ion stages required for efficient in band EUV emission, resulting in poor conversion efficiency (CE). For these reasons, it is desirable to find a technique to remove the tail and also to tune the length of the pulse in order to improve the CE to EUV radiation. The shortened pulses, if amplified, would also serve to generate plasmas with a higher electron temperature. Moving to shorter wavelength sources for lithography beyond 13.5 nm, amplified, short CO_2 pulses could be used to excite plasmas containing gadolinium for 6.76 nm sources.[4]

Several methods of producing shortened CO_2 laser pulses have been previously demonstrated,[5–14] with varying degrees of complexity and success. Earlier techniques relied on focusing the laser pulse in a background gas to form a plasma shutter.[5–7] Plasma formation occurs at a definite time during the laser pulse and the remaining part of the pulse is

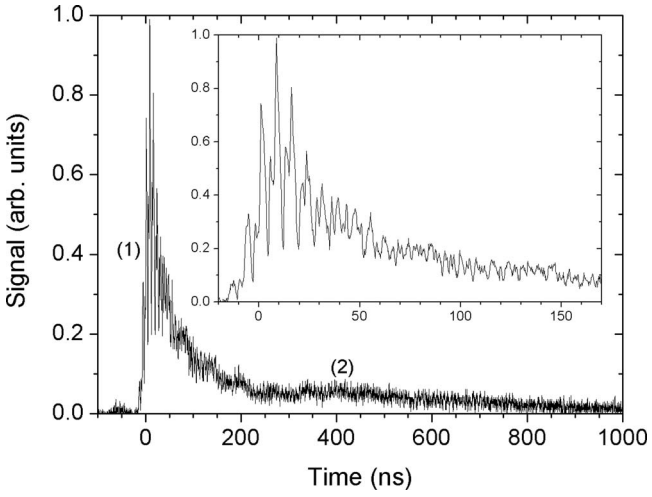

FIG. 1. Temporal profile of a TEA CO_2 laser pulse showing the two temporal components; a short intense first peak (1) followed by a second low energy long duration peak (2). The graph inset shows a close up of the first peak.

absorbed in the plasma thus modifying the pulse length. Further development of this simple technique followed which saw the addition of an electrical discharge[8,9] or a second laser pulse[10] to aid breakdown in the background gas. These procedures are limited to low repetition rates due to the background gas renewal time and control of spatial stability can be an issue. Q-switched pulse shortening[11,12] has also been demonstrated, but the output energies need to be small to avoid damage to optical components. Short pulse production by mode locking[13] schemes also suffer from this drawback. Very recently, an aluminium pinhole target plasma shutter[14] has been demonstrated where plasma is formed around the periphery of the pinhole. Lateral expansion of the plasma renders the pinhole opaque to the laser and shortens the pulse length of the output laser beam. The minimum reported duration achieved with these techniques, with the exception of Q-switched and mode locked pulses, is 10 ns.[8]

In this paper, we present a simple plasma shutter device that is capable of shortening TEA CO_2 pulses down to 2 ns. The pulse shortening principle is demonstrated and verified using a simple laser heating model. The technique is free from both precision timing and alignment requirements.

II. EXPERIMENT

The TEA-CO_2 laser used in these experiments is an Optosystems Infralight SP10 gas flow laser system. The operating wavelength is 10.6 μm and the total energy output can vary depending on the ratio of the laser gas mix ($He:N_2:CO_2$) used and the discharge voltage, which can vary from 10 to 27 kV. Energies from 0.1 to 1.7 J can be achieved, with varying temporal profiles. Throughout the experiment presented here the laser was operated with a standard gas mix of 6:1:3 and 27 kV. This produced output energy of around 1.2 J with a typical laser pulse temporal profile shown in Fig. 1. Due to losses at several optical components the on-target laser energy

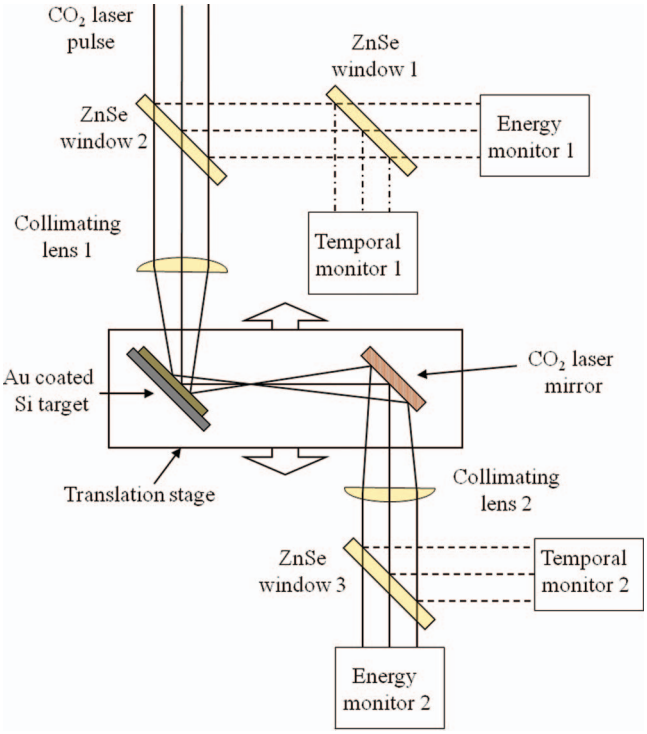

FIG. 2. (Color online) Experimental setup for production of a plasma shutter for CO_2 laser pulse shortening. A highly reflective target is placed close to the focus of two collimating lenses. Temporal and energy monitors measure the laser pulse duration and energy before and after the plasma shutter. The entire setup is placed in vacuum to avoid air breakdown at or close to the laser focus.

was ~1 J. The entire pulse is around 1.5 μs in duration and the FWHM for the initial peak is estimated to be 50 ns. To estimate the laser power density, the laser pulse profiles were smoothed to remove the oscillating structure.

The laser pulse to be shortened entered a collimating lens configuration where a 500 nm thick gold-coated silicon target was placed close to the collimator focus. The experimental setup is shown in Fig. 2 (not drawn to scale). The target was placed at 45° to the incident laser. Motorized stages and actuators were used to move the target within the lens collimator setup to change the focused laser spot size on the reflective gold target and thus change the applied power density. A CO_2 laser mirror was then used on the same translation stage to direct the beam to the second lens of the fixed optical collimator. ZnSe windows were placed in the beam path before and after the plasma shutter which acted as 98:2 beam splitters for *in situ* measurement of the laser pulse energy and temporal profile. The beam energy was measured using calibrated energy monitors and the temporal profiles were recorded using infrared photon drag detectors with rise-times of ≈1 ns. Error in timing measurements using these detectors is also ~1 ns. The target setup is maintained under vacuum with a chamber pressure of 5×10^{-6} mbar. The variation of the laser spot size as a function of target position was measured separately using a scanning knife edge technique[15] for accurate estimation of the focused laser spot from which the on-target power density was found.

III. RESULTS AND DISCUSSION

For dense low temperature plasmas far infrared radiation is efficiently absorbed by inverse bremsstrahlung due to the λ^3 dependence of this process.[16,17] For high laser power density (CO_2, $> 10^9$ W cm^{-2}), a plasma is always produced very early during the laser pulse. The remainder of the laser pulse is strongly coupled into this plasma inducing significant heating and ionization. If the applied power density is lowered to a value close to the ablation threshold, then plasma formation does not take place until later in the irradiation process. Before plasma formation occurs the laser pulse can be efficiently reflected from the metal surface. Thus, the plasma formation time can be controlled by adjusting the power density. In the present work, this was achieved by moving the target very precisely with respect to the laser focus.

An example of the reflected CO_2 laser pulses obtained are presented in Fig. 3, showing four reflected pulses, as well as the laser pulse measured before shortening, for increasing power density. In Fig. 3(a), the applied power density is below the ablation threshold and the metal film acts as a mirror. As the power density is increased plasma is formed and efficiently absorbs the remaining part of the laser pulse, including the low energy long duration tail. This can be seen in Fig. 3(b). Increasing the power density still further results in earlier plasma formation and therefore a shorter duration reflected pulse as shown in Fig. 3(c). Eventually, the power density becomes so high that very little of the incident pulse is reflected (Fig. 3(d)). A scan of the variation of pulse duration with incident power density was performed by moving the target position relative to the focus of the beam collimator. Close to the laser focus a short pulse length is observed which increases in length the further from the focus that the target is located. The variation of pulse duration with power density is shown in Fig. 4. For a power density below 2.5 $\times$ 10^7 W cm^{-2} there is no pulse shortening, indicating that this value is close to the plasma formation threshold. In the power density range 2.5 $\times$ 10^7–1.0 $\times$ 10^8 W cm^{-2}, the laser pulse is shortened from 50 to 10 ns. Increasing the power density beyond this value shortens the pulse further down to a minimum value of ≈2 ns at 1.8 $\times$ 10^8 W cm^{-2}.

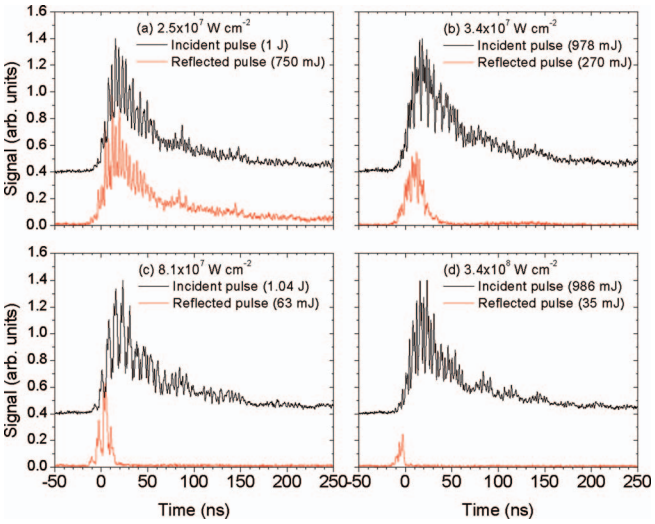

FIG. 3. (Color online) Temporal profile of the reflected pulses during laser irradiation of Au for different laser power densities (a) 2.5 $\times$ 10^7 W cm^{-2} (b) 3.4 $\times$ 10^7 W cm^{-2} (c) 8.1 $\times$ 10^7 W cm^{-2} (d) 3.4 $\times$ 10^8 W cm^{-2}. The incident pulse profile is shown on top in black, in each panel and the corresponding reflected pulse is shown below it in red (grey).

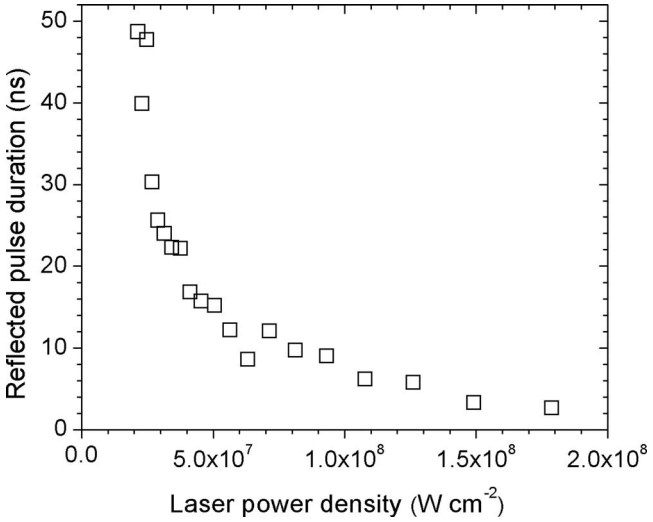

FIG. 4. Variation of reflected pulse duration as a function of applied laser power density.

The variation of total reflected energy corresponding to the pulse durations given in Fig. 4 was also measured and is shown in Fig. 5. For incident power densities below the plasma formation threshold almost all of the incident energy is reflected. As the power density is increased, the reflected energy is reduced by plasma absorption. For a power density of 3.4 $\times$ 10^7 W cm^{-2} (Fig. 3(b)), 270 mJ is reflected in a pulse of duration 22 ns. At 8.1 $\times$ 10^7 W cm^{-2} (Fig. 3(c)), 63 mJ is reflected in 10 ns, while at the minimum pulse duration measured of 2.5 ns the energy reflected from the target was measured to be 35 mJ. For fixed conditions the shortened pulse duration and energy varies on a shot to shot basis but this is due to the variation of the initial input pulse from the TEA CO_2 laser. The variation is ∼±10% for longer pulse durations (≈10–50 ns) and less than ±20% for shorter pulse durations (<10 ns). Of interest for experiments investigating EUV and x-ray emission in LPPs is the instantaneous power and the ability to focus to power densities >10^9 W cm^{-2}. For $\lambda = 10.6\ \mu$m and short focal length optics (e.g., f = 5 cm) typical focused spot diameters of the Infralight SP10 laser used in these experiments were around 200 μm. For laser power densities greater than 10^9 W cm^{-2}, this requires the instantaneous power to be greater than 1 MW. The reflected laser pulse power as a function of incident power density is also shown in Fig. 5. For all pulse durations, the reflected power is larger than 1 MW and in most cases exceeds it by an order of magnitude, and is sufficient for generation of hot plasma for EUV emitting sources with the added ability to change the laser pulse duration to optimize conditions for EUV conversion efficiency.

To explore the mechanisms responsible a simple laser heating model[18] was used to explain the behavior of the plasma shutter. The model assumes heating of a semi-infinite,

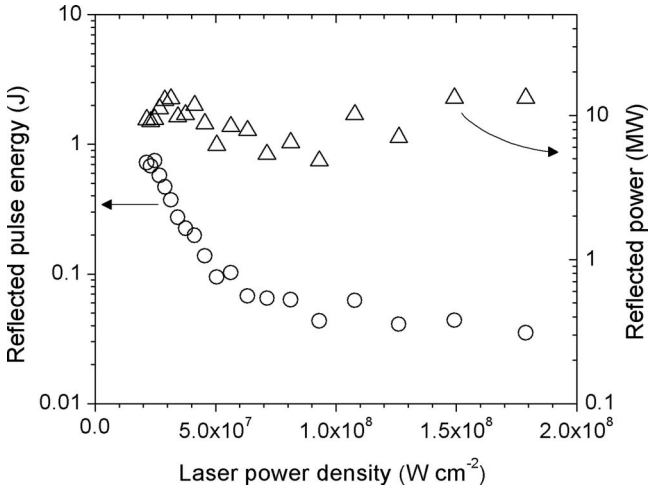

FIG. 5. Variation of reflected pulse energy and total reflected power as a function of applied laser power density.

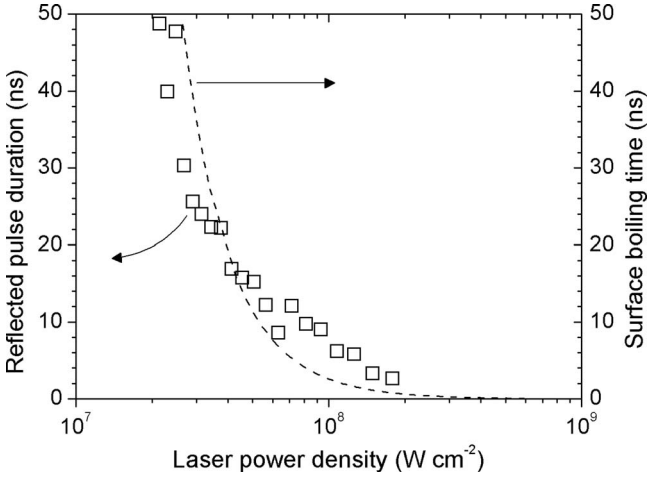

FIG. 6. Comparison of the measured reflected pulse durations (square symbols) and the calculated boiling times (dashed line) as a function of laser power density.

homogeneous, and isotropic metallic sample by a laser pulse with a rectangular (i.e., top-hat) temporal profile. Solving the heat conduction equation[18,19] gives an analytic expression for the temperature distribution during the laser pulse, inside the metal target, $T(z,t)$ as

$$T(z,t) = \left(\frac{2(1-R)I_0}{\rho C}\right)\sqrt{\frac{t}{\kappa}}\,ierfc\left[\frac{z}{z(\kappa t)^{1/2}}\right] + T_i. \quad (1)$$

In the above equation, I_0 is the laser intensity, R is the target reflectivity at the laser wavelength, ρ is the density, C is the specific heat capacity, and $\kappa = (k/\rho C)$ is the thermal diffusivity (k being the thermal conductivity). T_i is the initial temperature. The *ierfc* function is described in Ref. 19. At the surface (i.e., z = 0), Eq. (1) reduces to the following:

$$T(0,t) = \left(\frac{2(1-R)I_0}{\rho C}\right)\sqrt{\frac{t}{\pi\kappa}} + T_i. \quad (2)$$

The above equation is valid for laser heating when the target remains in the solid state. When laser heating is sufficient to induce surface melting, Eq. (2) becomes

$$T(0,t) = \left(\frac{2(1-R)I_0}{\rho C}\right)\sqrt{\frac{t}{\pi\kappa}} + T_i - T_q, \quad (3)$$

where $T_q = q/C$, where q is the latent heat of melting. The operation of plasma shutter induced pulse shortening depends on the plasma formation time during laser irradiation. If we consider that the plasma formation time is approximately equal to the time it takes for the surface temperature to reach the boiling point, then Eq. (3) can be used to predict the plasma formation time and thus the reflected pulse duration, as a function of laser power density. Rearranging Eq. (3) gives

$$t_B = \pi\kappa\left[\left(\frac{\rho C}{2(1-R)I_0}\right)(T_B - (T_i - T_q))\right]^2, \quad (4)$$

where t_B is the time it takes for the surface temperature to reach the boiling point and T_B is the boiling temperature of the metal. Using Eq. (4) above with the room temperature, bulk thermal properties of Au,[20] t_B can be estimated as a function of power density. This is shown in Fig. 6 and compared to the reflected pulse duration measurements. The thermal properties used in the calculation are shown in Table I.

The calculated boiling times show the same general trend as observed for the measured pulse durations with increasing power density. The measured pulse duration and calculated boiling time both drop from 50 ns to less than 10 ns with one order of magnitude increase in power density. However, the power density range where the calculated boiling time is comparable to the shortened pulse durations is significantly larger for the calculated values. For the comparison shown in Fig. 6, the calculated values were shifted to lower power density to overlap the experimental values. There are several reasons that higher calculated power density values are required to reproduce the experimental trend. Hot spots are present in the beam and the experimental intensity is averaged over the fluctuations evident in Fig. 1. Taking these factors together leads to spatial and temporal instantaneous values of power density significantly in excess of the average. Second, the laser heating model assumes a semi-infinite slab, whereas for this experiment Au thin films of ~500 nm thickness deposited on Si were used as reflective targets. The heat penetration depth, $l_{th} = (\kappa\tau_p)^{1/2}$ for our laser is about 2.5 μm, taking the pulse duration as 50 ns. This is significantly larger than the Au layer thickness. As the thermal conductivity of Si is half that of Au the heat conduction away from the target surface is

TABLE I. Material properties of bulk Au used in the laser heating calculation. The thermal properties of Au at room temperature (300 K) were used.

Bulk room temperature properties of Au	
Specific heat (C)	130 (J kg^{-1} K^{-1})
Thermal conductivity (k)	315 (W m^{-1} K^{-1})
Thermal diffusivity (κ)	1.28 × 10^{-4} (m^2 s^{-1})
R @ 10 600 nm	0.9
Latent heat of melting (q)	6.3 × 10^4 (J kg^{-1})
Density (ρ)	19 300 (kg m^{-3})
Melting temperature (T_m)	1337 (K)
Boiling temperature (T_B)	3129 (K)

larger in the model thus underestimating the surface temperature rise. Third, the thermal conductivity of gold at 1400 °C is almost one third of that at room temperature, leading to a faster temperature rise than predicted by the model. Including the temperature dependence of the thermal parameters in the laser heating model is difficult and numerical solutions are required. The comparison of this simple laser heating model was not meant as a rigorous quantitative treatment but rather to examine the link between the laser heating dynamics and the reflected pulse duration. From the comparison it can be clearly seen that the reflected pulse duration is directly dependent on the plasma formation time which can be controlled by adjusting the applied laser power density.

The major drawback of this technique is that after each pulse shortening event a new ablation site must be used as the reflective coating is destroyed at the point of laser incidence. Once the metal coating is removed the target must be changed. For continuous operation of this shutter a regenerating, liquid metal-coated target will be used in place of the gold-coated silicon target. This technology, developed at our research group in UCD, is described in Ref. 21 and is being implemented for realization of a continuous operation plasma shutter with the characteristics described in this article. In the near future these shortened pulses will be deployed in studies to optimize the CE from CO_2 irradiated pre-formed laser plasmas.

IV. CONCLUSION

We have demonstrated a simple plasma shutter for shortening the pulse duration of a TEA CO_2 laser and for removal of the long lived, low energy tail. We used a highly reflective target surface to reflect the pulse and through careful choice of our laser intensity, a timed plasma shutter was produced that modified the pulse length. The method produces short pulse durations in the range 2–50 ns and compares very well with respect to what has been previously reported by other methods, including cost of production. By employing a regenerative target to reflect the pulse, a reusable pulse shortening device can be produced.

ACKNOWLEDGMENTS

This work was supported by Science Foundation Ireland under Grant No. 07/IN.1/I1771.

[1] *EUV Sources for Lithography*, edited by V. Bakshi (SPIE Press, Bellingham, WA, 2006).
[2] J. White, P. Dunne, P. Hayden, F. O'Reilly, and G. O'Sullivan, Appl. Phys. Lett. **90**, 181502 (2007).
[3] H. Mizoguchi, T. Abe, Y. Watanabe, T. Ishihara, T. Ohta, T. Hori, A. Kurosu, H. Komori, K. Kakizaki, A. Sumitani, O. Wakabayashi, H. Nakarai, J. Fujimoto, and A. Endo, Proc. SPIE **7636**, 763608 (2010).
[4] T. Cummins, T. Otsuka, N. Yugami, W. Jiang, A. Endo, B. Li, C. O'Gorman, P. Dunne, E. Sokell, G. O'Sullivan, and T. Higashiguch, Appl. Phys. Lett. **100**, 061118 (2012).
[5] Y. Qua, X. Hua, D. Rena, Bo Zhoua, and W. Song, Proc. SPIE **4914**, 273 (2002).
[6] T. Gasmi, H. A. Zeaiter, G. Ropero, and A. G. Urena, Appl. Phys. B **71**, 169 (2000).
[7] H. S. Kwok and E. Yablonovitch, Opt. Commun. **21**, 252 (1977).
[8] C. Bellecci, I. Bellucci, P. Gaudio, S. Martellucci, G. Petrocelli, and M. Richetta, Rev. Sci. Instrum. **74**, 1064 (2003).
[9] J. Knittel, D. P. Schemer, and F. K. Kneubuhl, IEEE J. Quantum Electron. **32**, 2058 (1996).
[10] Y. Tao, M. S. Tillack, N. Amin, R. A. Burdt, S. Yuspeh, N. M. Shaikh, and F. Najmabadi, Rev. Sci. Instrum. **83**, 123503 (2009).
[11] A. W. Pasternak, D. J. James, J. A. Nilson, D. K. Evans, R. D. McAlpine, H. M. Adams, and E. B. Selkirk, Appl. Opt. **20**, 3849 (1981).
[12] H. Hoshino, T. Suganuma, T. Asayama, K. Nowak, M. Moriya, T. Abe, A. Endo, and A. Sumitani, Proc. SPIE **6921**, 692131 (2008).
[13] H. Houtman and J. Meyer, Opt. Lett. **12**(2), 87 (1986).
[14] N. Hurst and S. S. Harilal, Rev. Sci. Instrum. **80**, 035101 (2009).
[15] J. M. Khosrofian and B. A. Garetz, Appl. Opt. **22**, 3406 (1983).
[16] Y. B. Zel'dovich and Y. P. Raizer, *Physics of Shock Waves and High Temperature Hydrodynamic Phenomena* (Dover, New York, 2002).
[17] R. Jordan and J. G. Lunney, Appl. Surf. Sci. **127–129**, 941 (1998).
[18] V. N. Tokarev and A. F. H. Kaplan, J. Appl. Phys. **86**, 2836 (1999).
[19] A. M. Prokhorov, *Laser heating of metals* (Taylor & Francis, London, 1990).
[20] Y. S. Touloukian, *Thermophysical properties of high temperature solid materials* (Collier-MacMillan, New York, 1967).
[21] K. Fahy, F. O'Reilly, E. Scally, and P. Sheridan, Proc. SPIE **7802**, 78020K (2010).